Journal of Physics:
Conference Series

PAPER • **OPEN ACCESS**

In-situ measurement method for large-scale underwater equipment based on dehazing imaging technology

To cite this article: Shoubo Zhao 2025 *J. Phys.: Conf. Ser.* **3023** 012006

In-situ measurement method for large-scale underwater equipment based on dehazing imaging technology

Shoubo Zhao[1,2,3*]

[1]School of Mechanical Engineering, Guangdong Ocean University, Guangdong Engineering Technology Research Center of Ocean Equipment and Manufacturing, Zhanjiang 524088, China
[2]Shenzhen Institute of Guangdong Ocean University, Shenzhen 518120, China
[3]Guangdong Provincial Engineering Technology Research Center for Marine Equipment and Manufacturing, Zhanjiang 524088, China;

[*]Corresponding author's e-mail: shoubozh@126.com

Abstract: In-situ measurement for large-scale underwater equipment has been confronted with many challenges in measuring distance and accuracy. Existing methods can only detect small equipment with meter level dimensions. Inspired by indoor global positioning system (IGPS) measurement technology of large-scale equipment on land, we propose a underwater dehazing imaging three-dimensional measurement method based on digital micro-mirror device (DMD) sparse sensing to settle above issues. Specifically, polarization dehazing imaging involves modulating conjugated scattering field to eliminate background scattered light from water propagation. The multi frequency sonar locator builds underwater IGPS by obtaining the distances of spherical transmitters. The experiments demonstrate that the accuracy of combined measurement reaches 1mm with a measurement distance of 100 meters. This method is suitable for measuring the deformation of large underwater equipment such as dam gates, ships, and pipelines

1. Introduction

Large-scale underwater equipment has been used in shipping manufacturing and marine energy engineering. In-situ measurement for large-scale underwater equipment is essential[1]. Measuring the deformation of ship components is a typical example in the final assembly inspection process of ships. Welding processes, construction environments, and construction technique all affect the mechanical properties of ship panels. Once the weight of the ship's hull changes, the ship's hull will deform. By measuring the deformation of ship panels, quality issues during the manufacture process can be promptly perceived to improve the overall structural strength and service life of the ship. Additionally, ship panels and blades will undergo plastic deformation when they are subjected to underwater impact stress. The measurement on blades' deformation is also a crucial means of assessing navigation safety and optimizing ship performance. Currently, numerical simulation methods such as finite element analysis (FEA) are widely used to predict the deformation trends of ship hull grillages, in order to optimize process parameters and minimize deformation[2,3]. The accuracy of these methods is affected by various factors, such as model precision, mesh quality, boundary condition settings and solver performance. These factors can lead to discrepancies between analysis results and reality.

The data collected through in-situ measurements are significantly more believable than those generated by numerical simulation methods. However, large-scale underwater measurements face significant challenges due to the limitations of light propagation in water. Water media have stronger optical properties of light absorption and scattering, which seriously interfere with underwater optical imaging. According to Lambert's law and Rayleigh's law, light attenuation with various degrees occurs under the water. As a result, the optical illumination distance and imaging distance have been significantly reduced, severely limiting the visual spatial measurement range. Moreover, underwater scattering reduces the accuracy of image sensor. The low contrast and resolution of the image is manifested by white parasitic images and ghosting, which blur the image[4].

Large-scale in-situ measurement technology has attracted significant attention from both domestic and international researchers due to its critical role in various scientific and engineering fields. Researchers have explored the use of computer vision for large-scale in-situ measurement, leveraging advancements in imaging technology and image processing algorithms. Techniques such as binocular vision and structured light measurement have been widely studied and applied[5]. Researchers abroad have continuously improved vision-based measurement systems, integrating artificial intelligence and machine learning algorithms to enhance the accuracy and robustness of these systems[6].Laser-based measurement systems, including laser trackers and laser scanners, have been developed to achieve high precision and efficiency in large-scale in-situ measurements. These systems are capable of capturing large amounts of data rapidly and accurately[7].Ultrasonic measurement techniques have also been researched for their potential in large-scale in-situ measurement. However, the accuracy of these techniques can be affected by factors such as surface roughness and environmental temperature[8].The above methods are more common in onshore measurements and cannot effectively solve the limitations of underwater measuring range and accuracy.

Polarized imaging exploits the uniqueness and differences in the polarization information of scattered light fields to analyze the polarization characteristics of targets and backgrounds. By accurately estimating the polarization properties of target information light and background scattered light, and their relationships and differences, polarized imaging can effectively remove background scattered light to achieve clear underwater imaging[9,10]. Polarized imaging technology not only enhances imaging quality but also enables rapid detection, identification, and three-dimensional reconstruction of deformation. To overcome above limitations, we combine polarization dehazing imaging, laser scanning and sonar positioning to enhance underwater measuring range and accuracy. Combined measurement can leverage the point cloud measurement advantages of laser scanner and the long-distance measurement advantages of sonar locator, achieving high-precision measurement over a large range

Our group has been conducting long-term research on (Digital Micromirror Device) DMD cameras and measurement methods[11-12]. By utilizing spatial light modulators, which are controlled by driving electrical signals, we can alter the direction, amplitude, phase, wavefront, and polarization state of light in space. This enables the image sensing matrix to possess rich information about the measured target such as the spectrum, dynamic range, size, texture, light field. The visual sensing system perceives the characteristics of the measured target before image formation to enhance the signal and suppress the noise. To meet in-situ measurement requirements of large-scale underwater equipment, we propose a underwater dehazing imaging three-dimensional measurement method based on DMD sparse sensing.

This paper is organized as follows: Section2 describes our proposed metrology including polarization dehazing imaging, laser scanning and combined measurement. Section3 demonstrates the performance of experiments about dehazing imaging, combined measurement and measurement uncertainty. Section4 concludes this paper.

2. Metrology

2.1. Polarization dehazing imaging

The system consists of laser, polarizers, beam split, 4f beam expanders, DMD, micro polarizer array

(MPA), and camera, as shown in Figure 1. The 532nm laser beam is polarized into linearly polarized light that vibrates perpendicular to each other, passing through a polarizer and being transmitted onto the DMD. MPA decomposes the reflected polarization at different angles, and the camera records the light intensity in each polarization direction. Reflected light carries scattering field information affected by water propagation. According to scattering field distribution, DMD is controlled as a conjugate modulation field to eliminate scattering components. The Jones matrix is expressed as follows:

$$c\begin{bmatrix} J_{11} & J_{12} \\ J_{21} & J_{22} \end{bmatrix} = \begin{bmatrix} 1 & 1 \\ 1 & -1 \end{bmatrix}\begin{bmatrix} X_{11} & 0 \\ X_{21} & 0 \end{bmatrix} + \begin{bmatrix} 1 & -1 \\ 1 & 1 \end{bmatrix}\begin{bmatrix} 0 & X_{12} \\ 0 & X_{22} \end{bmatrix} \tag{1}$$

Where c is the normalization coefficient, the minimum power attenuation ratio for a light wavelength of 532nm is given by:

$$\alpha_{\lambda} = 1 - cI_0 \tag{2}$$

Equation1 is also a matrix representation of polarization, aiming to eliminate liquid optical rotation phenomenon from the polarization characteristics of light and underwater scattering theory. Underwater equipment is clearer due to elimination of scattering components. Under the condition of minimum energy attenuation, the farthest imaging distance can be achieved.

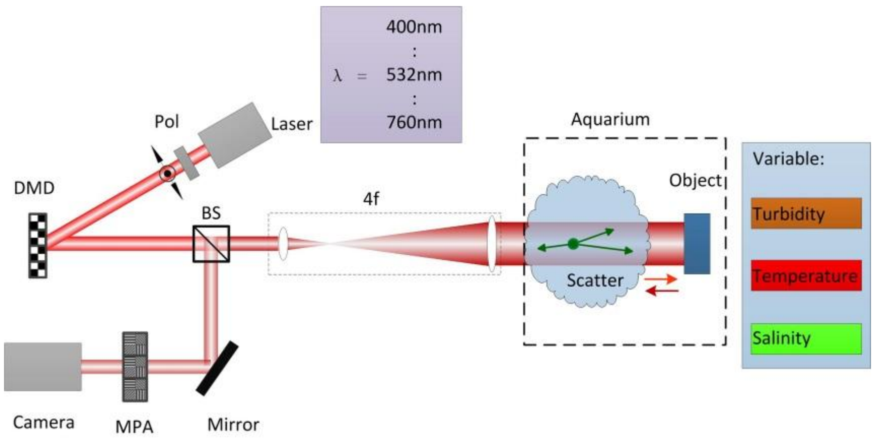

Figure 1. Polarization dehazing imaging system.

2.2. Laser scanning

Laser Scanner is a phase measurement device that employs a line structured light source to illuminate the object. The surface contour of the object modulates the projected light. The modulated light is captured by a polarization dehazing imager. Based on the principle of similar triangles, laser scanning utilizes the stripe deformation on the measured surface to calculate the distance of points from reference plane. The actual height H of a point P on the object's surface can be expressed as:

$$H = l \cdot \Delta\varphi / (2\pi d) \tag{3}$$

Where l is the distance from the projection center to the reference plane, $\Delta\varphi$ is the phase difference between the projected grating and the distorted grating captured by the camera at point P, and d is the distance between the projection center and the camera center. To obtain the absolute height, the reference plane must be calibrated to establish a baseline. This involves the mapping from the height and the phase values of the reference plane points in the camera.

2.3. Combined measurement

The proposed method is a combined measurement based on a laser scanner and a sonar locator, as shown in Figure 2. The multi-frequency sonar locator and the laser scanner move synchronously under the water. The laser scanner collects the three-dimensional coordinates of the surface points of the measured target on the cooperative coordinate system. Spherical transmitters O, X, Y, Z mounted on laser scanner build a cooperative coordinate system. Spherical transmitter O serves as the origin of the cooperative coordinate system. The direction from spherical transmitter O to spherical transmitter X is the x_c axis direction, the direction from spherical transmitter O to spherical transmitter Y is the y_c axis direction, and the direction from spherical transmitter O to spherical transmitter Z is the z_c axis direction. Spherical transmitters O, X, Y, and Z simultaneously emit sonar signals of different frequencies. These signals are received by the multi frequency sonar locator. The multi frequency sonar locator obtains the three-dimensional coordinates of spherical transmitter O, spherical transmitter X, spherical transmitter Y, and spherical transmitter Z in the world coordinate system by recognizing sonar signals. The three-dimensional coordinates of the surface points of the measured target on the world coordinate system $O(x_w^O, y_w^O, z_w^O)$, $X(x_w^X, y_w^X, z_w^X)$, $Y(x_w^Y, y_w^Y, z_w^Y)$ and $Z(x_w^Z, y_w^Z, z_w^Z)$ are obtained through coordinate transformation.

The cosine values of the angles between the x_c, y_c, and z_c axes in the cooperative coordinate system and the x_w, y_w, and z_w axes in the world coordinate system are calculated respectively.

$$\begin{cases} \cos < x_c, x_w >= (x_w^X - x_w^O) / \sqrt{(x_w^X - x_w^O)^2 + (y_w^X - y_w^O)^2 + (y_w^X - y_w^O)^2} \\ \cos < y_c, x_w >= (x_w^Y - x_w^O) / \sqrt{(x_w^Y - x_w^O)^2 + (y_w^Y - y_w^O)^2 + (y_w^Y - y_w^O)^2} \\ \cos < z_c, x_w >= (x_w^Z - x_w^O) / \sqrt{(x_w^Z - x_w^O)^2 + (y_w^Z - y_w^O)^2 + (y_w^Z - y_w^O)^2} \\ \cos < x_c, y_w >= (y_w^X - y_w^O) / \sqrt{(x_w^X - x_w^O)^2 + (y_w^X - y_w^O)^2 + (y_w^X - y_w^O)^2} \\ \cos < y_c, y_w >= (y_w^Y - y_w^O) / \sqrt{(x_w^Y - x_w^O)^2 + (y_w^Y - y_w^O)^2 + (y_w^Y - y_w^O)^2} \\ \cos < z_c, y_w >= (y_w^Z - y_w^O) / \sqrt{(x_w^Z - x_w^O)^2 + (y_w^Z - y_w^O)^2 + (y_w^Z - y_w^O)^2} \\ \cos < x_c, z_w >= (z_w^X - z_w^O) / \sqrt{(x_w^X - x_w^O)^2 + (y_w^X - y_w^O)^2 + (y_w^X - y_w^O)^2} \\ \cos < y_c, z_w >= (z_w^Y - z_w^O) / \sqrt{(x_w^Y - x_w^O)^2 + (y_w^Y - y_w^O)^2 + (y_w^Y - y_w^O)^2} \\ \cos < z_c, z_w >= (z_w^Z - z_w^O) / \sqrt{(x_w^Z - x_w^O)^2 + (y_w^Z - y_w^O)^2 + (y_w^Z - y_w^O)^2} \end{cases} \quad (4)$$

Laser scanner collects the three-dimensional coordinates of the surface point $P(x_c^P, y_c^P, z_c^P)$ of the measured target on the cooperative coordinate system. The cooperative coordinate of the surface point $P(x_c^P, y_c^P, z_c^P)$ is converted into three-dimensional coordinates on the world coordinate system $P(x_w^P, y_w^P, z_w^P)$ as follows:

$$\begin{bmatrix} x_w^P \\ y_w^P \\ z_w^P \end{bmatrix} = \begin{bmatrix} \cos < x_c, x_w > & \cos < y_c, x_w > & \cos < z_c, x_w > \\ \cos < x_c, y_w > & \cos < y_c, y_w > & \cos < z_c, y_w > \\ \cos < x_c, z_w > & \cos < y_c, z_w > & \cos < z_c, z_w > \end{bmatrix} \begin{bmatrix} x_c^P \\ y_c^P \\ z_c^P \end{bmatrix} + \begin{bmatrix} x_w^O \\ y_w^O \\ z_w^O \end{bmatrix} \quad (5)$$

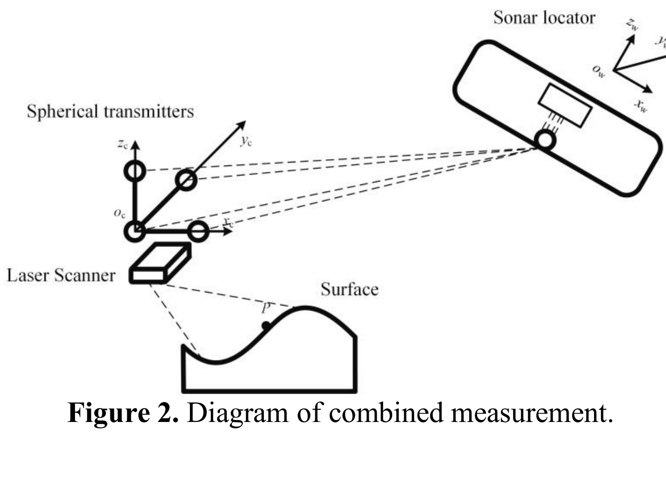

Figure 2. Diagram of combined measurement.

3. Experiment

The experimental site is in waters near Zhanjiang. The resolution of the camera is 10 million pixels. The underwater measurement accuracy of the laser scanner is 0.5mm, with a measurement distance of 2m and a measurement depth of 3m. The measurement accuracy of sonar locator within a measurement range of 100m is 0.5m. The experiment including dehazing imaging, combined measurement and measurement uncertainty are conducted, as shown in Figure 3. In Fig.3(a), star as the imaging object is immersed in muddy water. Polarization dehazing imaging system based on DMD sparse sensing removes the parasitic image to enhance clarity. Mean square errors (MSE) and Peak Signal-to-noise ratios (PSNR) of dehazing images with various attenuation coefficients are presented in Table 1. Fig.3(b) are the reconstructed 3D shape from point cloud in combined measurement. In the combined measurement experiment, sonar locator tracks laser scanner within a range of 100m. Laser scanner captures 3D data of Large-scale underwater equipment through free movement. Underwater pipeline and marine engine turbine blade have been successfully obtained using the proposed method.

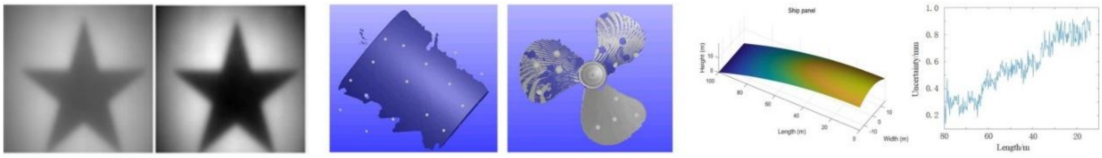

(a) (b) (c)

Figure 3. The experimental results of (a) dehazing imaging, (b) combined measurement and (c) measurement uncertainty.

Table 1. MSEs and PSNRs of dehazing images with various attenuation coefficients

Attenuation coefficient	0.051m-1	0.210m-1	0.331m-1
MSE	0.4946	0.5867	0.6063
PSNR	42.2243	42.0178	41.9431

According to Equation 5, uncertainty of combined measurement is calculated as follows:

$$\begin{bmatrix} U_x & U_y & U_z \end{bmatrix}^T = \begin{bmatrix} \partial\Theta/\partial x_c & & \\ & \partial\Theta/\partial y_c & \\ & & \partial\Theta/\partial z_c \end{bmatrix} \begin{bmatrix} \Delta_x & \Delta_y & \Delta_z \end{bmatrix}^T + \begin{bmatrix} \mathrm{O}_x & \mathrm{O}_y & \mathrm{O}_z \end{bmatrix}^T \quad (6)$$

Where $\begin{bmatrix} U_x & U_y & U_z \end{bmatrix}^T$ is the global measurement uncertainty. $\begin{bmatrix} \Delta_x & \Delta_y & \Delta_z \end{bmatrix}^T$ is the uncertainty of laser scanner. $\begin{bmatrix} \mathrm{O}_x & \mathrm{O}_y & \mathrm{O}_z \end{bmatrix}^T$ is the uncertainty of sonar locator. Θ is the first term of Equation 5. The global accuracy is determined by the uncertainties of laser scanner and sonar locator. A perfect strategy would optimize the scanning action to minimize the partial differentiation of Θ. Three-dimensional data of ship panel under impact stress is compared with standard panel to obtain the measurement uncertainty of proposed method, as shown in Fig.3(c). The nominal values of ship panel are from the point measurement of laser tracker on land. The combined uncertainty is defined by the difference between the nominal value and experimental results. The measurement uncertainty comprises two factors: systematic uncertainty and random uncertainty. Determined by Θ, systematic uncertainty is manifested as an increasing trend with distance. Random uncertainty is manifested as the degree of data dispersion. According to above theoretical analysis and experimental results, the global measuring accuracy of proposed method reaches 1mm with a measurement distance of 100 meters.

4. Conclusion

Proposed underwater dehazing imaging three-dimensional measurement method, leveraging DMD sparse sensing and inspired by state-of-the-art polarized imaging technology, has demonstrated significant potential in addressing the challenges associated with in-situ measurement of large-scale underwater equipment. By utilizing polarization dehazing to modulate and eliminate background scattered light, combined with a laser scanner employing line structured light, the method achieves accurate point cloud acquisition in a cooperative coordinate system. Furthermore, the integration of a multi-frequency sonar locator facilitates the determination of the relationship between the cooperative and world coordinates, ensuring the practical application of the method in real-world underwater environments. Experimental results validate the effectiveness and robustness of the proposed approach, making it a promising solution for high-precision measurements of large-scale underwater equipment.

This paper focuses on the in-situ measurement for large-scale underwater equipment. The next task is to use this method to analyze deformation of ship panels when they are subjected to underwater impact stress. The deformation is related to the magnitude, position, and angle of underwater impact stress. Our proposed method is suitable for measuring various responses to deformation.

Acknowledgments
This work was supported in part by the National Natural Science Foundation of China under Grant 61801148, the University Nursing Program for Young Scholars with Creative Talents in Heilongjiang Province under Grant UNPYSCT-2020187 and the program for scientific research start-up funds of Guangdong Ocean University under Grant 060302062301.

References
[1] Rahman S., Li A.Q., Rekleitis I., SVIn2: A multi-sensor fusion-based underwater SLAM system[J]. International Journal of Robotics Research, 2022, 41(11-12): 1022-1042.
[2] Ramajeyathilagam K., Vendhan C. P., Deformation and rupture of thin rectangular plates subjected to underwater shock[J]. International Journal of Impact Engineering, 2004, 30(6): 699-719.
[3] Suresh C., Ramajeyathilagam K., Large deformation behaviour of thin mild steel rectangular plates subjected to underwater explosion loading under air and water backed conditions[J]. Applied Ocean Research, 2021, 114: 10278.
[4] Peng L. T., Zhu C. L., Bian L. H., U-Shape transformer for underwater image enhancement[J]. IEEE Transactions on Image Processing, 2023, 3: 3066-3079.
[5] Border R., Gammell J. D., The surface edge explorer (SEE): A measurement-direct approach to next best view planning[J]. International Journal of Robotics Research, 2024, 43(10): 1506-1532
[6] Lemos R., Cabral R., Ribeiro D., and so on. Automatic Detection of Corrosion in Large-Scale Industrial Buildings Based on Artificial Intelligence and Unmanned Aerial Vehicles[J]. Applied Sciences-Basel, 2023, 13(3): 1386.
[7] Zhuang Y., Jiang N., Hu H. S., and so on. 3-D-Laser-Based Scene Measurement and Place Recognition for Mobile Robots in Dynamic Indoor Environments[J]. IEEE Transactions on Instrumentation and Measurement, 2013, 62(2), 438-450.
[8] Zhang C. B., Cheung C. F., Liang X. L., and so on. Ultrasonic vibration-assisted sculpturing of large-scale 3D optical microstructure arrays with small theoretical error and reliable dynamic response[J]. Precision Engineering, 2024, 89: 262-275.
[9] Schechner Y.Y., Karpel N., Recovery of underwater visibility and structure by polarization analysis[J]. IEEE Journal of Oceanic Engineering, 2005, 30(3): 570-587.
[10] Treibitz T., Schechner Y.Y., Active Polarization Descattering[J]. IEEE Transactions on Pattern Analysis and Machine Intelligence, 2009, 31(3): 385-399.
[11] Zhao S. B., Yang Y. Q., Three-dimensional shape measurement for the steep surface using DMD camera[J]. Scientific Reports, 2022, 12(1): 21054.
[12] Zhao S. B., Liu L. Y., Ma M. Y., Adaptive high-dynamic range three-dimensional shape measurement using DMD camera[J]. IEEE Access, 2019, 7: 67934-67943.